

# Disk emission and atmospheric absorption lines in black hole candidate 4U 1630-472

A. Róžańska<sup>1</sup>, J. Madej<sup>2</sup>, P. Bagińska<sup>1</sup>, K. Hryniewicz<sup>1</sup>, and B. Handzik<sup>2</sup>

<sup>1</sup> N. Copernicus Astronomical Center, Bartycka 18, 00-716 Warsaw, Poland  
e-mail: agata@camk.edu.pl

<sup>2</sup> Warsaw University Observatory, Al. Ujazdowskie 4, 00-478 Warsaw, Poland  
e-mail: jm@astrouw.edu.pl

Received ????, .....; accepted ???, .....

## ABSTRACT

**Context.** We re-analyzed SUZAKU data of the black hole candidate 4U 1630-472 being in the high/soft state. The source, known for X-ray outbursts and for absorption dips, has X-ray continuum spectrum well interpreted as an accretion disk emission. Additionally, two absorption lines from He and H-like iron were clearly detected in 4U 1630-472 high resolution X-ray data.

**Aims.** We show that the continuum X-ray spectrum of 4U 1630-472 with iron absorption lines can be satisfactorily modeled by the spectrum from an accretion disk atmosphere. Absorption lines of highly ionized iron originating in hot accretion disk atmosphere can be an alternative or complementary explanation to the wind model usually favored for these type of sources.

**Methods.** We perform full radiative transfer calculations to model the emission from an accretion disk surface which is seen at different viewing angles using our transfer code ATM21. Computed models are then fitted to high resolution X-ray spectra of 4U 1630-472 obtained by SUZAKU satellite.

**Results.** We model continuum and line spectra using a single model. Absorption lines of highly ionized iron can origin in upper parts of the disk atmosphere which is intrinsically hot due to high disk temperature. Iron line profiles computed with natural, thermal and pressure broadenings match very well observations.

**Conclusions.** According to any global disk models considered for the mass of central object of the order  $10 M_{\odot}$  or less, the effective temperature of the inner radii reaches  $10^7$  K. We showed that the accretion disk atmosphere can effectively produce iron absorption lines observed in 4U 1630-472 spectrum. Absorption line arising in accretion disk atmosphere is the important part of the observed line profile, even if there are also other mechanisms responsible for the absorption features. Nevertheless, the wind theory can be an artifact of the fitting procedure, when the continuum and lines are fitted as separate model components.

**Key words.** X-rays: binaries, Stars: individual, Accretion, accretion disks, Radiative transfer, Line: profiles,

## 1. Introduction

Emission from the accretion disk around a compact object is the commonly accepted model for the soft X-ray bump observed in Galactic Black Hole candidates (GBHc). Depending on the mass of the central object and on the accretion rate, the inner disk temperature for the black hole of  $10 M_{\odot}$  can be of the order of  $10^7$  K (Róžańska et al. 2011b). According to the accretion disk theories, either geometrically thin, optically thick standard disk (Shakura & Sunyaev 1973, hereafter SS disk), even with relativistic corrections (Novikov & Thorne 1973, hereafter NT disk), or slim disk (Abramowicz et al. 1988), temperature always increases with decreasing mass of the central object and increasing accretion rate.

For such high temperatures of an accretion disk atmosphere, thermal lines from H-like and He-like iron ions should be formed, and those lines should be visible between 6.7 to 9.2 keV, where the latter value is energy of the last iron bound-free transition (from H-like ion to complete ionization). Nevertheless, it is well known that observed X-ray spectra from compact binaries not always exhibit disk component. Due to instrument's technical limits and due to spectral state transition, multi-temperature disk component may not be detected in full X-ray energy range. To explain data by the accretion disk emission we have to be sure

that observations were taken when the source was in so called “soft state” - dominated by disk-like component.

Recently, several X-ray binaries do exhibit absorption lines from highly ionized iron (Boirin et al. 2004; Kubota et al. 2007; Díaz Trigo et al. 2012). Many of those sources show dips in their light curves, which are believed to be caused by obscuration of the central X-ray source by a dense material located at the outer edge of an accretion disk. Such obscuring material was accumulated during accretion phase from the companion star onto the disk (White & Swank 1982). The presence of dips and lack of total X-ray eclipses by the companion star indicate that the system is viewed relatively close to edge-on, at an inclination angle in the range  $\sim 60 - 80^\circ$  (Frank et al. 1987).

He-like and H-like Fe absorption features indicate that highly ionized plasma is present in these systems. Study of these lines is extremely important to characterize the geometry and physical properties of plasma. Recently, it was shown that the presence of absorption lines is not necessarily related to the viewing angle since non-dipping sources also show those features (Díaz Trigo et al. 2012). Moreover, the FeXXV absorption line was also observed during non-dipping intervals in XB1916-053 (Boirin et al. 2004).

Usual way of modeling highly ionized Fe absorption lines from those sources at first is to fit continuum to the spectrum, given either by multi-blackbody disk emission or by powerlaw

Send offprint requests to: A. Róžańska

shape. After fitting of the continuum each line is fitted separately using Gaussian shape. In such a way, equivalent widths (EWs) and velocity shifts of the line centroid can be derived. In most cases absorbing material is outflowing with velocities reaching few hundred km/s. The extreme example is the recent observation of black hole candidate IGR J17091-3624, where the wind velocity was estimated as  $0.03 c$  (King et al. 2012). Additionally, photoionisation modeling can be done using grid of models computed by `xSTAR` (Kallman & Bautista 2001) if the quality of spectrum is good enough. Nevertheless, this is always done after continuum fitting is established, and usually at least two or more photoionised slab components are needed to model all lines (King et al. 2012). In case of black hole transient IGR J17091-3624, EWs of Fe<sub>xxv</sub> and Fe<sub>xxvi</sub> lines are approximately twice bigger when fitting `xSTAR` models, than simple the Gaussian shape.

In this paper, we present alternative analysis of *Suzaku* XIS X-ray spectra of 4U 1630-472 presented in Kubota et al. (2007). Instead of multi-blackbody disk emission `DISKBB` with two Gaussians fitted separately, we used our atmospheric disk emission models (`ATM`) recently computed and published in Róžańska et al. (2011b). Our theoretical spectra were obtained from careful radiative transfer computations in accretion disk atmospheres. All calculations of continuum and line spectra were performed simultaneously, taking into account relativistic Compton scattering of X-ray photons. Absorption profiles of Fe<sub>xxv</sub> and Fe<sub>xxvi</sub> spectral lines were carefully computed as a convolution of natural, thermal (Gaussian) and pressure broadenings. Expressions describing pressure broadening of iron lines were deduced from considerations by Griem (1974). In the case of our models lines are fitted together with underlying continuum.

The paper is organized as follows: Sec. 2 describes recent observational status of Fe absorption lines in X-ray binaries, Sec. 3 explain principal assumptions of our theoretical model. All the procedure of data reduction and spectral fitting which were done by us is presented in Sec. 4. Conclusions and discussion are formulated in Sec. 5.

## 2. Narrow Fe absorption lines in X-ray binaries

Different types of X-ray binaries exhibit presence of narrow absorption lines from highly ionized iron. Tab. 1 is an updated version of the Table 5 from Boirin et al. (2004). In the past research most of objects were fitted using `POWERLAW` model to describe continuum, and Gaussian shape for lines. In some sources, being in soft state (i.e. dominated by the disk component) multi-temperature disk black body model (`DISKBB`), and Voigt profiles for individual lines (`KABS`) were considered (Kubota et al. 2007).

Gaussian profile fitted to an individual absorption line puts constrains on the ionic column density. Such ionic column densities can be incorporated with photoionisation calculations to derive ionization parameter and total column density of absorbing material. In case of X-ray binaries, photoionisation models show  $N_H$  of the order of  $10^{23-24} \text{ cm}^{-2}$  with the value of ionization parameter  $\xi = 10^{3-4}$ . Such estimates were obtained for a few systems, assumed to be highly inclined

Usually prominent  $K_\alpha$  absorption lines from He and H-like iron are detected with EWs from -5 up to -61 eVs (minus sign denotes an absorption line). Only in few systems  $K_\beta$  lines are visible. The extreme case is XB1916-053, in which He-like iron line changes its EW during the persistent and dipping time intervals. In persistent phase,  $EW = -30_{-12}^{+8}$ , while during dipping phase the equivalent width changes from  $EW = -74_{-27}^{+20}$

to  $EW = -168_{-46}^{+44}$  (Boirin et al. 2004). Summary of the objects with absorption lines and the connection of EWs with spectral state is shown in Ponti et al. (2012).

In GX 13+1 properties of the absorber do not vary strongly with the orbital phase, which suggests that ionized plasma has a cylindrical geometry. Therefore, inclination of GX 13+1 was constrained between 60-80°. Note, that almost all values of inclinations in fourth column of Tab. 1 were not known before the discovery of iron absorption lines in those sources. Adopting wind geometry, the presence of Fe absorption lines suggests high inclination of those sources. This is the reason why inclination numbers in fourth column are so similar.

Properties of the absorption features in GX 13+1, and MXB 1659-298 show no obvious dependence on the orbital phase, except during a dip from X1624-490, where there is an evidence for the presence of additional colder material. Boirin & Parmar (2003) have modeled narrow absorption features of Fe<sub>xxvi</sub>  $K_\alpha$  and  $K_\beta$  during non-dip intervals. Therefore, ionized absorption features may be common characteristics of disk accreting systems. Systems with shorter orbital periods are expected to have smaller accretion disks.

In XB 1323-619 a number of absorption lines (6.7 and 6.9 keV) were discovered in non-dip, non-burst spectra (Church et al. 2005). Curve of growth analysis provided a consistent solution in which line ratio was reproduced assuming collisional ionization with  $kT=31$  keV, close to the accretion disk corona (ADC) electron temperature in this source. Thus, Church et al. (2005) proposed that those absorption lines in the dipping low mass X-ray binaries (LMXB) are produced in ADC.

From observational point of view ADC can produce the same spectral features like upper layers of accretion disk atmosphere. Temperature of both emission regions can be comparable as we explain in the following Sections.

## 3. Fe absorption lines in accretion disk atmosphere

In this paper, we fitted the few iron rich model disk atmospheres, which were already computed and presented in Róžańska et al. (2011b) to the *Suzaku* X-ray spectra of 4U 1630-472. Since the observed iron lines in 4U 1630-472 were discovered in absorption, we use only non-irradiated modeled disk spectra.

Full simulation of emission from accretion disk atmospheres is very time consuming and depends on the assumed global disk model. The code used in this paper was fully described in our previous paper Róžańska et al. (2011b). We remind here the most essential properties of our numerical approach. The accretion disk at a given accretion rate and black hole spin is divided on approximately 15 rings. At each ring we computed local model atmosphere using complete and consistent radiative transfer code `ATM21` (Róžańska & Madej 2008). The code assumes that the vertical optical depth at some standard photon frequency is the independent variable in the model. At the fixed chemical composition model atmosphere assumed two parameters: the effective temperature, which at each ring was determined from the accretion rate, and the gravity in vertical direction caused by the black hole for the given mass. Each model atmosphere was strongly non-gray, and the local emissivity or opacity was a sum of non-gray bound-free, free-free, and bound-bound absorption/emission caused by individual ions. Moreover, local opacity and emissivity was influenced by Compton scattering by free electrons. We always assumed that a single local electron temperature is valid for all processes, also those including ions. Velocity distribution of all particles is relativistic and Maxwellian.

**Table 1.** Measured absorption line properties and orbital parameters of sources with observed Fe absorption lines, L - LMXB, microq - micro-quasars, D - deeps, E - eclipses, B - bursts, qB - quasi-periodic bursts, T - transient, O - outburst, J - radio jet.

Source	ref.	Type	$P_{orb}(h)$	$i(^{\circ})$	Fexxv $K\alpha$ E (keV) EW (eV)	Fexxvi $K\alpha$ E (keV) EW (eV)	Fexxv $K\beta$ E (keV) EW (eV)	Fexxvi $K\beta$ E (keV) EW (eV)
XB 1916-053 (NS)	[1]	LMXB D, B	0.8	60 – 80	$6.65^{+0.05}_{-0.02}$ $-30^{+8}_{-12}$	$6.95^{+0.05}_{-0.04}$ $-30^{+11}_{-12}$	$7.82^{+0.03}_{-0.07}$ (a) $-21^{+9}_{-12}$	$8.29^{+0.08}_{-0.12}$ $-19^{+11}_{-12}$ eV
GX 13+1 (NS)	[2]	LMXB Atol, B	577.4	60 – 80 (b)	$6.75^{+0.02}_{-0.05}$ $-20 \pm 5$	$7.02 \pm 0.06$ $-41 \pm 7$	$7.91^{+0.46}_{-0.15}$ $-33 \pm 12$	$8.24^{+0.04}_{-0.06}$ $-37 \pm 15$
MXB 1659-298 (NS)	[3]	LMBX D, E, T	7.1	~ 80	$6.64 \pm 0.02$ $-33^{+9}_{-20}$	$6.90^{+0.02}_{-0.01}$ $-42^{+8}_{-13}$	– –	– –
X 1254-690 (NS)	[4]	LMXB D	3.9	60 – 80	– –	$6.95 \pm 0.03$ $-27^{+11}_{-8}$	– –	$8.20^{+0.05}_{-0.10}$ $-17 \pm 9$
X 1624-490	[5]	LMXB D	20.9	60 – 80	$6.72 \pm 0.03$ $-7.5^{+1.7}_{-6.3}$	$7.0 \pm 0.02$ $-16.6^{+1.9}_{-5.9}$	– –	– –
XB 1323-619	[6]	LMXB D, qB	2.93	60 – 80	$6.70 \pm 0.03$ $-22 \pm 3$	$6.98 \pm 0.04$ $-27 \pm 4$	– –	– –
Cir X-1 (NS)	[7]	B, D, O, J	398	high	$6.701 \pm 0.009$	$6.965 \pm 0.01$	–	–
4U 1630-472 (BH)	[8]	LMXB D, T, O	690	~ 70	$6.72 \pm 0.01$ $-21 \pm 3$	$6.980^{+0.009}_{-0.007}$ $-30^{+2}_{-3}$	$7.84^{+0.04}_{-0.03}$ $-18.2^{+4}_{-6}$	$8.11^{+0.05}_{-0.06}$ $-15.8^{+5}_{-7}$
GRO J1655-40 (BH)	[9]	microq D, O	62.9 (c)	69 – 85	$6.63 \pm 0.07$ $-61^{+15}_{-13}$	$6.95 \pm 0.10$ $-25^{+13}_{-11}$	$7.66 \pm 0.13$ $-35^{+30}_{-29}$	– –
	[10]				$6.698 \pm 0.001$ $-45.59 \pm 1.8$	$6.999 \pm 0.002$ $-30.82 \pm 2.37$	$7.842 \pm 0.005$ $-48.11 \pm 4.46$	$8.277 \pm 0.01$ $-27.63 \pm 5.53$
GRS 1915+105 (BH)	[11]	microq	804	~ 70	$6.72^{+0.015}_{-0.017}$ $-35.8^{+3.7}_{-7.8}$	$7.000^{+0.020}_{-0.014}$ $-43.2^{+6.3}_{-5.3}$	$7.843^{+0.037}_{-0.035}$ $-30.8^{+11.2}_{-5.8}$	$8.199^{+0.065}_{-0.064}$ $-22^{+11}_{-12}$
	[12]				$6.684 \pm 0.022$ $-6$	$6.984 \pm 0.009$ $-18$	– –	– –
H1743-322 (BH)	[13]	microq D, T, O	–	~ 70	$6.709 \pm 0.004$ $-5 \pm 1$	$6.981 \pm 0.004$ $-20 \pm 2$	– –	– –
IGR J17091-3624 (BH)	[14]	T, O	–	–	$6.91 \pm 0.01$ $-21^{+0.5}_{-0.2}$	$7.32^{+0.01}_{-0.06}$ $-32^{+1.8}_{-0.4}$	– –	– –

[1] - XMM, Boirin et al. (2004), [2] - XMM, Ueda et al. (2001); Díaz Trigo et al. (2012), [3] - XMM, Sidoli et al. (2001), [4] - XMM, Boirin & Parmar (2003), [5] - XMM, Parmar et al. (2002), [6] - XMM, Church et al. (2005), [7] - *Chandra*, Brandt & Schulz (2000), [8] - SUZAKU epoch 4 Kubota et al. (2007), [9] - ASCA, Ueda et al. (1998) [10] - *Chandra*, Miller et al. (2008), [11] - ASCA, Kotani et al. (2000), [12] - *Chandra*, Lee et al. (2002), [13] - *Chandra* epoch 1, Miller et al. (2006), [14] - *Chandra*, King et al. (2012),

(a) - Identified as Sxvi and Nixxvii transitions by Boirin et al. (2004)

(b) - Low  $i$  suggested by high radio to X-ray ratio (Schnerr et al. 2003), but high  $i \simeq 60 - 80^{\circ}$  by detection of Fe abs. lines (Díaz Trigo et al. 2012)

(c) - From optical observations (Orosz & Bailyn 1997)

We numerically simulated emission assuming radial effective temperature distribution for slim disk model (Abramowicz et al. 1988) as the most reasonable one. Nevertheless, calculations of  $T_{eff}(R)$  for the standard SS disk (Shakura & Sunyaev 1973) or for NT disk (Novikov & Thorne 1973) give similar results, as was shown in Fig. 1 by Róžańska et al. (2011b). In all cases, for the mass of black hole  $M_{BH} = 10M_{\odot}$  and for high accretion rate, temperature in the inner disk can reach  $10^7$  K. This temperature even rises when spin of the black hole increases.

The whole disk was divided into individual rings and at each distance from the black hole full radiative transfer computations were done assuming that the atmosphere is in radiative and hydrostatic equilibrium. We use our code for model atmosphere computations, ATM21, suitable for computing disk vertical structure and its X-ray intensity spectra. Compton scattering on free electrons and ionization structure were self consistently taken into account (Madej & Róžańska 2004). Final spectrum of the disk was obtained by integrating of contributions from individual rings.

In particular our X-ray model spectra included profiles of eight most prominent lines from highly ionized iron. Those lines belong to two fundamental series of iron. Helium-like iron FeXXV produces the resonant line at  $E=6690$  eV, commonly denoted as 6.7 keV, and three lines at energies:  $E=7881$ , 8226, and 8416 eV. The series of hydrogen-like iron FeXXVI consists of the resonant line at  $E=6898$  eV and higher lines at  $E=8172$ , 8621, and 8829 eV.

Additionally, we include three bound-free edges: FeXXIV edge at  $E = 8690$  eV, FeXXV edge at  $E= 8829$  eV, and FeXXVI edge at  $E=9278$  eV, which are visible in high energy X-ray band. These are ionization energies from the innermost K-shell. Other iron edges, which were included in our computations arise from all K, L, M shells, but we do not list them since they are not prominent above 2 keV.

Róžańska et al. (2011b) have shown that in galactic black hole binaries, accretion disk must be very hot, with local effective temperatures approaching  $10^7$  K on the innermost orbits. In such high temperatures iron is almost fully ionized and spectral features of helium and hydrogen-like resonant iron lines must play a crucial role in interpreting of the observed GBHB spectra in soft state.

Therefore, iron absorption lines, which were observed recently in disk dominated binaries, see section above, most likely are resonant lines from upper layers of accretion disk atmospheres. In our models we take into account all three line broadening mechanisms: natural, thermal (Gaussian) and pressure broadening. Broadened iron line profiles were carefully computed as the convolution of all three partial broadenings.

Tab. 2 presents theoretical equivalent widths of resonant lines computed in our radiative transfer simulations (Róžańska et al. 2011b). All were computed only for five sets of global disk parameters and for eight viewing angles. In all cases mass of the black hole was assumed to be equal  $10M_{\odot}$ , nevertheless we do not have mass estimation in 4U 1630-472. Models do not cover all values in the parameter space, but in this paper for the first time we present fitting to the 4U 1630-472 absorption lines together with underlying continuum.

Note, that theoretical EWs are usually not very high, and only for the hottest model the ratio of EWs for FeXXV and FeXXVI lines is of the order of 2 (four leftmost columns in Tab. 2). For other models the atmospheric temperature is too low to produce prominent hydrogen-like iron line. In future work we plan to compute the whole grid of disk atmosphere models and make them suitable for spectral fitting.

## 4. Suzaku observations of 4U 1630-472

### 4.1. The source

Black hole candidate 4U 1630-472 is known for X-ray outbursts that repeat within roughly 600-690 days (Jones et al. 1976; Parmar et al. 1995). The source has been observed by many major X-ray missions, showing heavy absorption with  $N_H = 5 - 12 \times 10^{22} \text{ cm}^{-2}$  (Tomsick et al. 1998). X-ray absorption dips observed in this source suggest large inclination angle around  $60^\circ$  (Kuulkers et al. 1998). This conclusion was based on the model where dips are produced during eclipse of accretion disk corona (ADC) by warm bulge, which develops when matter falls from companion star on the outer rim of the disk.

No optical counterpart is known for 4U 1630-472 mostly due to its large reddening and location in a crowded star field (Parmar et al. 1986). Therefore, the distance and mass of the compact object in 4U 1630-472 are unknown and the source is

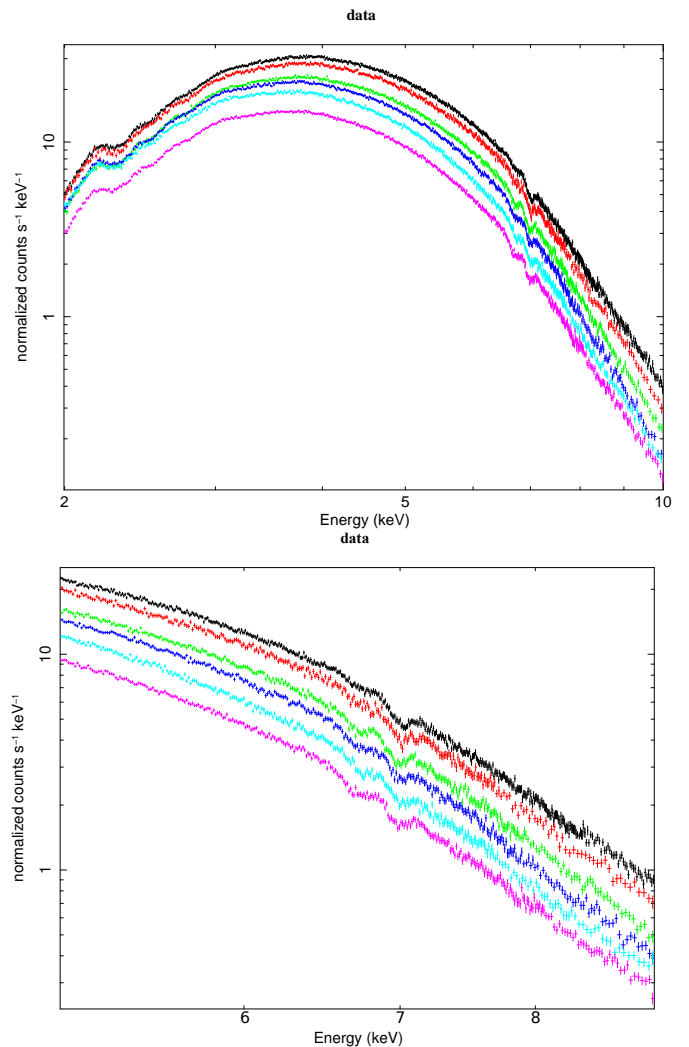


**Fig. 1.** X-ray spectra of 4U 1630-472 obtained with the XIS023 showing prominent bump similar to multi-temperature disk emission - upper panel. Lower panel is a focus on the iron line region from 5-9 keV, where absorption features are clearly seen. Colors mean different epochs of observations starting from black - epoch 1, up to magenta - epoch 6. The data are very similar to those presented in Kubota et al. (2007) in Fig.2 and Fig.5.

classified as a black hole, due to the similarity of its X-ray spectral and timing properties to those shown by systems with measured black hole masses.

Recent *Suzaku* monitoring of the source led to successful detection of absorption lines in all six observations (Kubota et al. 2007). Lines were interpreted as an absorption in the wind. In this paper we show that this is not the only one interpretation. By fitting iron absorption lines produced in outer regions of the accretion disk and hot atmosphere, together with underlying continuum, we demonstrate that existing satellites are not able to distinguish between both models. The model of outflowing wind with velocity of the order of hundred km/s fits as well as the model of static atmospheres. Our analysis also suggests that the wind can originate from hot accretion disk atmosphere.

**Table 2.** Equivalent widths of the model iron line components (in eV): FeXXV and FeXXVI resonant lines for five sets of the couple of parameters  $\dot{m}$  and spin  $a$ . All EWs are given for viewing angles from  $i = 11.4^\circ$  (face-on disk), to  $i = 88.9^\circ$  (edge-on disk). In the first row we put global parameters of a model: accretion rate  $\dot{m}$  in units of Eddington accretion rate, and dimensionless black hole spin  $a$ .

inc.( $^\circ$ )	$\dot{m}=0.01$	$a=0.98$	$\dot{m}=0.1$	$a=0.98$	$\dot{m}=0.01$	$a=0$	$\dot{m}=0.1$	$a=0$	$\dot{m}=1$	$a=0$
	FeXXV	FeXXVI	FeXXV	FeXXVI	FeXXV	FeXXVI	FeXXV	FeXXVI	FeXXV	FeXXVI
11.4	-20.5	-10.5	-7.5	-3.6	-56.7	-1.7	-50.0	-1.7	-41.1	-9.7
26.1	-20.1	-10.3	-7.4	-3.5	-54.7	-1.6	-49.4	-1.8	-40.8	-9.5
40.3	-19.4	-9.9	-7.0	-3.1	-50.4	-1.4	-48.4	-1.8	-40.0	-9.1
53.7	-18.2	-9.3	-6.6	-2.7	-44.0	-1.1	-46.8	-1.9	-38.5	-8.8
65.9	-16.4	-8.4	-5.9	-2.1	-37.9	-0.9	-44.6	-2.0	-35.9	-8.6
76.3	-13.8	-7.5	-4.9	-1.6	-34.7	-0.8	-41.6	-2.2	-31.7	-8.9
84.2	-10.4	-6.3	-3.7	-1.2	-34.5	-0.7	-36.9	-2.6	-25.2	-9.8
88.9	-6.8	-4.7	-2.4	-1.1	-36.5	-0.6	-26.9	-4.3	-15.4	-10.6

#### 4.2. Data reduction

We have downloaded and reduced the same *Suzaku* data of 4U 1630-472 as those published by Kubota et al. (2007). Six observations were performed in time period from 08.02.2006 to 23.03.2006 after an outbursts that was reported in 12.2005 by *RXTE* ASM. The exact time of observations made by *Suzaku* in comparison with ASM lightcurve is marked in Kubota et al. (2007) Fig.1 by vertical arrows.

The source was observed by X-ray Imaging Spectrometer(XIS) operating in the 0.2 - 12 keV energy range, and one of two Hard X-ray Detectors (HXD), both instruments on the board of *Suzaku*. Nevertheless, for this analysis we took only XIS data. XIS is build out of four CCDs, located in the focal plane of X-ray mirrors (XRT). Three of those CCDs named: XIS0, XIS2, and XIS3 are front illuminated (FI), while XIS1 sensor is back illuminated (BI). In this paper we analyze both FI and BI CCD data. Due to high brightness of 4U 1630-472, XIS was set to 1/4 window option (which means we have 2 sec read out time) and first four observations were performed in burst option.  $2 \times 2$  and  $3 \times 3$  editing modes were used in observations. All exposure times and count rates are presented in Tab. 3.

In further analysis we used only  $3 \times 3$  editing mode data because  $2 \times 2$  data were not well calibrated during observation time. Although background was negligible during all 6 observations we subtracted it from the data. For extracting spectra from *Suzaku* filtered event file we used *xselect* - a HEASoft tool. Before extracting spectra or light curves in case of a point source we have to create circular extraction region centered on the sources. It is recommended to create regions which encircles 99 % of point source flux. In later reduction process we used *xissimarfgen* script to build response files for our spectra. *Xissimarfgen* is a generator of auxiliary response files (ARFs) that is based on ray-tracing and is designed for the analysis data from *Suzaku* XIS detectors. This script is calculating ARFs through Monte-Carlo simulations. The idea is that program ray-traces X-ray photons through the XRT and XIS and counts the number of events detected in extraction regions defined by user. We need to assume a sufficient number of photons to limit statistical errors to good level. In our analysis we assumed number of simulated photons to 400000 to minimize Poisson noise in ARFs. In order to carry out further analysis we downloaded redistribution matrix files (RMFs) from CALDB catalogs (for appropriate dates).

As we have created ARFs and collected all RMFs files, we used an ASCA tool called *addascaspec* to combine source

and background spectra and responses of *Suzaku* XIS0, XIS2, and XIS3 (FI chip) data. We also have tried to add all FI and BI (XIS1) chips despite that such a procedure was not recommended but we thought it can increase statistics in softer part of spectra.

We found out that over all six observations count rate declined through the time. We know that there is a count rate threshold above which data from the source can suffer from photon pileup effect. In case of point source, it is  $\sim 100$  counts/sq arcmin/s (CCD exposure) for *Suzaku* XIS instrument. In all six observations count rate for 4U 1630-472 was around 100 counts/sec., so we can assume both: that data have suffered from photon pileup or not.

To minimize pileup effect we have used two externally contributed routines *aeattcor.sl* and *pile\_estimate.sl*<sup>1</sup>. Both scripts are designed for the analysis of *Suzaku* data that might be affected by photon pile-up effect. Script *aeattcor.sl* improves the attitude correction for the slow wobbling of the optical axis for bright sources by using their detected image to create a new attitude file. Next, script *pile\_estimate.sl* is designed to be run just after *aeattcor.sl*. It creates an image that will show an estimated, minimum pile-up fraction for user specified levels. This allows us to create a region file that excludes the most piled areas, and then estimate the effective pile-up fraction of the remaining events.

But data with removed pile-up effect had much poorer statistics than those without removal, so in further modeling we have used not cleared data. 4U 1630-472 is near the threshold for pile-up, but we also can assume that there is no pile-up in those data as it was done by Kubota et al. (2007). All other data reduction and calibration uncertainties were done in the same way as in Kubota et al. (2007) paper. Extracted XIS spectra for six observations and the region of iron absorption lines are presented in Fig. 1. Final exposure time and count rate in each XIS CCD chip for each epoch of observation is presented in Tab. 3.

#### 4.3. Spectral fitting

Our numerical disk spectra (Róžańska et al. 2011b) were converted to the FITS format, suitable for XSPEC fitting package (version 12.6). Atmospheric models, hereafter named *ARM* were rare in parameter space. Since we do not know  $M_{BH}$ ,  $\dot{m}$  and  $a$  of the source, we took a prior set of parameters  $\dot{m}$  and  $a$  for a range of inclinations and fixed mass  $M_{BH} = 10M_{\odot}$ . We did not aim here to derive neither accretion rate nor spin of the black hole.

<sup>1</sup> <http://space.mit.edu/ASC/software/suzaku/>

**Table 3.** *Suzaku* observations of 4U 1630-472 for all 6 Epochs of the year 2006. Dates of observations are listed in the first column

Epoch	XIS	$T_{exp}$ [ks]	count rate
	0	11.08	$8.87E+01 \pm 8.95E-02$
1	1	11.06	$8.79E+01 \pm 8.92E-02$
Feb 8	2	11.02	$1.09E+02 \pm 9.94E-02$
	3	11.08	$1.28E+02 \pm 1.08E-01$
	FI	33.17	$1.02E+02 \pm 1.10E-01$
	FI+BI	44.23	$9.86E+01 \pm 7.60E-02$
	0	4.79	$7.48E+01 \pm 1.25E-01$
2	1	4.86	$7.37E+01 \pm 1.23E-01$
Feb 15	2	4.76	$9.06E+01 \pm 1.38E-01$
	3	4.79	$8.95E+01 \pm 1.37E-01$
	FI	14.34	$8.41E+01 \pm 8.09E-02$
	FI+BI	19.20	$8.13E+01 \pm 6.84E-02$
	0	10.7	$5.73E+01 \pm 7.32E-02$
3	1	10.71	$5.84E+01 \pm 7.38E-02$
Feb 28	2	10.64	$7.40E+01 \pm 8.34E-02$
	3	10.7	$6.71E+01 \pm 7.92E-02$
	FI	32.04	$6.51E+01 \pm 4.71E-02$
	FI+BI	42.75	$6.36E+01 \pm 4.00E-02$
	0	10.3	$5.87E+01 \pm 7.55E-02$
4	1	10.28	$5.30E+01 \pm 7.18E-02$
Mar 8	2	10.25	$6.54E+02 \pm 7.99E-02$
	3	10.3	$6.44E+02 \pm 7.91E-01$
	FI	30.85	$6.24E+01 \pm 4.68E-02$
	FI+BI	41.13	$5.99E+01 \pm 3.96E-02$
	0	5.24	$5.29E+01 \pm 1.01E-01$
5	1	23.18	$5.35E+01 \pm 4.80E-02$
Mar 15	2	5.24	$6.02E+01 \pm 1.07E-01$
	3	5.24	$5.82E+01 \pm 1.05E-01$
	FI	15.73	$5.65E+01 \pm 6.39E-02$
	FI+BI	38.9	$5.43E+01 \pm 3.91E-02$
	0	15.37	$4.45E+01 \pm 5.38E-02$
6	1	21.65	$4.64E+01 \pm 4.63E-02$
Mar 23	2	15.36	$5.33E+01 \pm 5.89E-02$
	3	15.36	$5.04E+01 \pm 5.73E-02$
	FI	52.37	$4.91E+01 \pm 3.40E-02$
	FI+BI	67.74	$4.81E+01 \pm 2.76E-02$

We for the first time fitted iron absorption line profiles different than simple Gaussian.

It was almost obvious that the best model is the hottest one, obtained for  $\dot{m} = 0.01$  in Edd. units and spin  $a = 0.98$ , since EWs of iron line were the biggest (see two leftmost columns in Tab. 2). After that, we were able to fit observations taking viewing angle as the only free parameter.

#### 4.3.1. Continuum

First, we performed fitting over the whole energy range 2-9 keV. Instead of using multi-temperature XSPEC model `DISKBB`, we applied our atmospheric disk emission `ATM` multiplied by interstellar absorption `WABS` model. Additionally we have added `POWERLAW` model to mimic possible influence of irradiation at hard part of the spectrum. From theoretical point of view, in sources being in soft state, dominated by disk emission, we expect that irradiation only slightly change hard tail of the disk spectrum. From instrumental point of view, high energy part can be affected by pile-up (see Sec. 4.2). In Kubota et al. (2007) this effect was modeled by a broad Gaussian in emission at 10 keV.

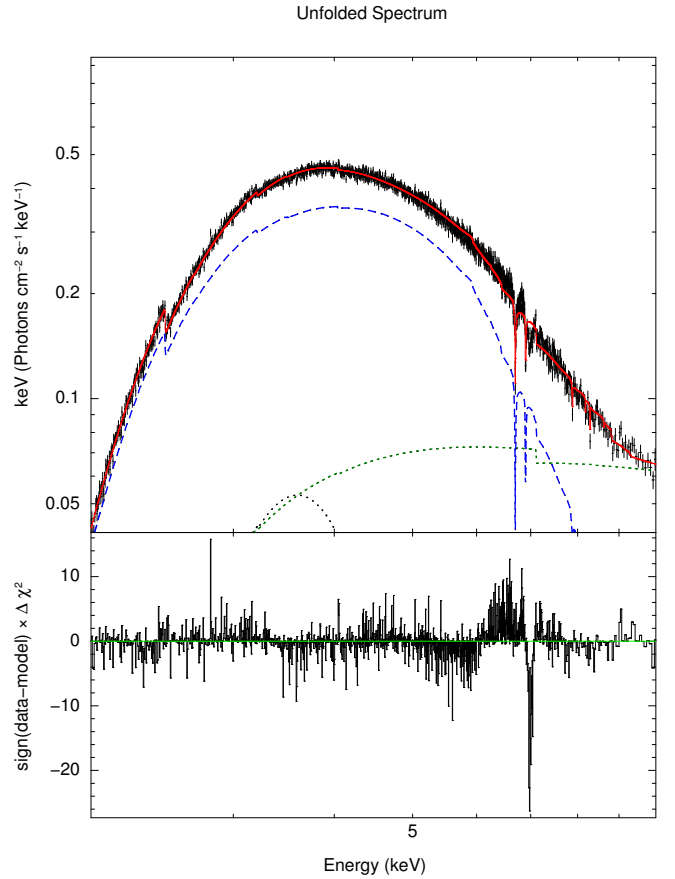


**Fig. 2.** Fitting of atmospheric disk model to the epoch 3 data in the range 2-9 keV. Observed data, black crosses, are a sum of three front illuminated (XIS0,2,3) and one back illuminated (XIS1) CCDs. The total model `WABS*(ATM+PL + GAUSSIAN)` is represented by red line. Separate model components are represented by long-dashed blue line - `ATM`, short-dashed green line - `PL`, and dotted black line - instrumental `GAUSSIAN`. Reduced  $\chi^2/d.o.f. = 2618.57/2182 = 1.2$  for the total model.

In our fitting procedure, the `POWERLAW` model with flat photon index should balance those two effects. Following suggestions made by Kubota et al. (2007) we have added Gaussian at  $\sim 3.2$  keV with width of the order of 0.1 keV to reduce systematic errors arising from current uncertainties in the instrument response at the gold M-II edge.

We point out here that our `ATM` atmospheric disk emission deviates from the multi-blackbody disk spectrum, since we took into account Compton scattering in hot disk atmosphere (Róžańska et al. 2011a). We did not assume anything about the total disk hardening factor. The effect of spectrum hardening is self consistently computed in our numerical model.

There are two ways to obtain high effective temperature in the inner rings of the accretion disk. First, high  $T_{eff}$  is the result of high accretion rate. This is quite obvious, higher accretion rate implies generation of higher flux of radiation especially in inner rings. Therefore, the value of accretion rate affects the most energetic part of the spectrum. The second way is to spin up black hole. If the black hole rotates than inner rings radiate more energy since the marginally stable orbit moves towards the black hole. Those rings are hot and, therefore, the total continuum spectrum looks as if the disk accreted at a high accretion rate. Additionally, disk spectra have slightly different shape for various viewing angles. To distinguish what particular spec-

**Table 4.** Fitting results of our atmospheric disk emission model to the 4U 1630-472 *Suzaku* data between 6-9 keV for the inclination angle  $i = 11 \pm 5^\circ$

Energy range 6-9 keV				
Ep.	WABS $N_H$ ( $10^{22}$ )	ATM Inc. (ang) Norm ( $10^{-5}$ )	PL Ph. Index Norm ( $10^{-3}$ )	$\chi^2/d.o.f.$
1	8	$11 \pm 5$ $2.9 \pm 0.6$	-0.7 $3.46 \pm 0.07$	2198.07/819 = 2.68
2	8	$11 \pm 5$ $2.04 \pm 0.02$	-0.7 $1.70 \pm 0.04$	1093.33/819 = 1.33
3	8	$11 \pm 5$ $1.96 \pm 0.48$	-0.7 $1.67 \pm 0.06$	1212.85/819 = 1.48
4	8	$11 \pm 5$ $1.76 \pm 0.46$	-0.7 $1.38 \pm 0.06$	1241.95/819 = 1.52
5	8	$11 \pm 5$ $1.17 \pm 0.48$	-0.7 $0.94 \pm 0.07$	793.06/819 = 0.97
6	$7.82 \pm 0.98$	$11 \pm 5$ $1.20 \pm 0.47$	$-0.24 \pm 0.27$ $3.16 \pm 0.2$	995.85/817 = 1.22

trum really fits the data we need much more models. For the 4U 1630-472 observed data favour the hottest model. However, we cannot claim about the accretion rate and black hole spin in this source. This is rather because absorption lines in such a model are the strongest and agree with observations.

Taking into account that the source 4U 1630-472 is covered by interstellar gas of high column density of the order  $8 - 9 \times 10^{22} \text{ cm}^{-2}$ , and the data were slightly affected by pile-up, we present continuum fitting only for Epoch 3 data. Each other set of observations gave similar results.

Fig. 2 presents our continuum fitting for Epoch 3 of FI+BI coadded spectra. The absorbing column density from interstellar gas was fitted to  $N_H = 8.23 \pm 0.08$ , which is consistent with previous fits. The best fitted atmospheric model gives inclination  $i = 11 \pm 5^\circ$  and normalization  $1.50 \pm 0.08 \times 10^{-5}$ . Additional POWERLAW photon index equals  $\Gamma = 1.48 \pm 0.55$ . In this fitting we didn't freeze any parameter. Our goodness of fit i.e.  $\chi^2$  per degrees of freedom is  $2618.57/2182 = 1.2$ .

#### 4.3.2. Iron line complex

For further analysis we decided to proceed fitting in the energy band restricted to the region of iron line complex i.e. between 6 and 9 keV. In that narrow band we still fit lines together with underlying continuum as a single model, ATM. We do not make any additional assumption to the line or edge profile, since all features are already build up in our radiative transfer calculations of atmospheric disk emission.

Since back illuminated XIS1 chip improves the statistics only in low energy tail around 2 keV or less, it should cause no difference in the range between 6-9 keV. Therefore, for further analysis we take only spectra from front illuminated - XIS023 chips, as it is in the paper by Kubota et al. (2007).

Choosing energy band between 6-9 keV we reduce number of degrees of freedom by a factor 2.5. We again fit WABS \* (ATM + POWERLAW) and results of this fitting are presented in Fig. 3. The importance of POWERLAW model is now lower than in case where fitting was done for full energy band (see Sec. 4.3.1). The photon index is usually  $-0.7 \pm 0.18$  and does not change much during different periods of observations. Similarly, column density of galactic interstellar absorption  $N_H$  in most cases equals  $8.16 \pm 0.12 \times 10^{22} \text{ cm}^{-2}$ . Since interstellar absorption should not change

**Table 5.** Fitting results of our atmospheric disk emission model to the 4U 1630-472 *Suzaku* data between 6-9 keV for the inclination angle  $i = 70 \pm 6^\circ$

Energy range 6-9 keV				
Ep.	WABS $N_H$ ( $10^{22}$ )	ATM Inc. (ang) Norm ( $10^{-5}$ )	PL Ph. Index Norm ( $10^{-3}$ )	$\chi^2/d.o.f.$
1	8	$70 \pm 6$ $4.78 \pm 0.03$	-0.7 $3.59 \pm 0.03$	2236.77/819 = 2.73
2	8	$70 \pm 6$ $3.347 \pm 0.032$	-0.7 $1.79 \pm 0.04$	1101.27/819 = 1.34
3	8	$70 \pm 6$ $3.253 \pm 0.024$	-0.7 $1.76 \pm 0.03$	1262.26/819 = 1.54
4	8	$70 \pm 6$ $2.915 \pm 0.023$	-0.7 $1.46 \pm 0.03$	1290.14/819 = 1.57
5	8	$70 \pm 6$ $1.957 \pm 0.024$	-0.7 $1.00 \pm 0.03$	796.61/819 = 0.97
6	$7.37 \pm 0.96$	$70 \pm 6$ $2.035 \pm 0.093$	$-0.7 \pm 0.18$ $1.20 \pm 0.08$	1033.43/817 = 1.26

in different Epochs we fixed this parameter at  $8 \times 10^{22} \text{ cm}^{-2}$ . Only for observation number 6 we allow interstellar absorption to vary, but fit is still with good statistics. We show all fitting parameters in Tables 4 and 5.

Again, all six spectra imply the inclination angle  $i = 11 \pm 5^\circ$ , since absorption lines in the disk seen “face on” are the deepest in our model. Nevertheless, we have checked if the disk observed at the viewing angle  $i = 70^\circ$ , appropriate for dipping sources can also explain observations. Surprisingly, fitting results with inclination frozen at  $70^\circ$  also give quite good statistics as seen (see Tab. 5).

Most important results of this paper are presented in Fig. 4, which is enlarged part of Fig. 3. Resonant helium and hydrogen-like iron lines are clearly seen with their complex profiles. Our absorption lines do not need any velocity shift, contrary to the previous analysis (Kubota et al. 2007). Absorption lines from the upper parts of static accretion disk atmosphere can also satisfactorily explain observations.

## 5. Conclusions

In this paper we presented fitting of complex continuum and line numerical models to X-ray spectra of 4U 1630-472. In our models the spectrum of disk emission was obtained from careful radiative transfer computations including Compton scattering on free electrons. The Fe line profiles are computed as the convolution of natural, thermal and pressure broadening mechanisms. The advantage of our models is that the continuum is fitted with lines simultaneously, which was never done before in the analysis of X-ray absorption lines seen in LMXBs. The usual procedure is to fit first the disk emission as a standard model in XSPEC fitting package, and Gaussian lines, where the energy of line centroid is a free parameter of fitting. In such the case, lines are usually blueshifted indicating that absorbing matter outflows. We show in this paper, that in the case of 4U 1630-472 there is sufficient to assume zero velocity shift of absorbing matter. In our paper iron absorption lines originate in the hot atmosphere above accretion disk.

Our models are parametrized only by mass of the black hole, its spin and disk accretion rate, which we assume to be constant at all radii. Since our computations are very time con-

suming and we have only few collected models, we are not able to derive those parameters from continuum fitting. On the other hand, quality of *Suzaku* data is high enough to follow the shape of continuum even in heavily obscured sources (in case of 4U 1630-472 obscuration due to Galactic absorption equals ca.  $8 \times 10^{22} \text{ cm}^{-2}$ ).

Accretion disk atmosphere spectra fits *Suzaku* data for 4U 1630-472 very well. The best fit we have obtained for the inclination angle  $i = 11^\circ$ . For higher angles i.e.  $i = 70^\circ$  fit is just slightly worse. This angle is within the range of inclination suggested in the literature taking into account dipping behavior and assuming absorption in the wind. Small difference of fit quality between different inclinations does not allow us to claim constraints on  $i$ .

Of course models such as `DISKBB+PL` plus absorption with two Gaussians always show better statistics than our more complex model. But the former model has many free parameters. This is a general rule that the more free parameters we have the more accurate is the final fit. The our model has no free parameters connected with lines, therefore, it has at least 6 parameters less than the set `DISKBB+PL` plus two Gaussians applied by Kubota et al. (2007).

According to any global disk models considered for the mass of central object of the order  $10 M_\odot$  or less, the effective temperature of the inner radii reaches  $10^7 \text{ K}$ . In such a case possible origin of absorption lines from accretion disk atmospheres should be taken into account in modeling of winds in X-ray binaries.

In the wind theory, it is widely accepted that the wind can be launched at the accretion disk surface. Upper layers of atmosphere can become unstable and start to blow out material due to radiation pressure. Our analysis does not contradict this fact, it rather shows that absorption at upper atmospheric layers cannot be distinguished from the absorption in the wind, which may be launched in the same region.

In this work we do not aim to tightly constrain parameters of the object but rather show that emission from the accretion disk atmosphere is an important mechanism which gives vital explanation or at least part of an answer to the question of origin of iron absorption in X-ray binaries.

The major conclusion of our analysis is that the shape of disk spectrum is well interpreted as 4U 1630-472 emission and that absorption lines do not need to set any velocity shift to explain data. Therefore, the wind explanation for absorbing matter is questionable and not unique. We showed that X-ray data of current quality can be interpreted in several ways and we cannot easily solve this ambiguity. We conclude that the wind theory can be an artifact of the fitting procedure, when the continuum and lines are fitted as separate model components. Data of higher spectral resolution are needed to discriminate between two models. Future satellites with calorimeters as *ASTRO-H* or *Athena+* will yield us the answer.

*Acknowledgements.* This research was supported by the Polish Ministry of Science and Higher Education grant No. N N203 511638, and by Polish National Science Center grant No. 2011/03/B/ST9/03281, and has received funding from the European Union Seventh Framework Program (FP7/2007-2013) under grant agreement No.312789.

## References

- Abramowicz, M. A., Czerny, B., Lasota, J. P., & Szuszkiewicz, E. 1988, *ApJ*, 332, 646  
 Boirin, L. & Parmar, A. N. 2003, *A&A*, 407, 1079  
 Boirin, L., Parmar, A. N., Barret, D., Paltani, S., & Grindlay, J. E. 2004, *A&A*, 418, 1061  
 Brandt, W. N. & Schulz, N. S. 2000, *ApJ*, 544, L123

- Church, M. J., Reed, D., Dotani, T., Bałucińska-Church, M., & Smale, A. P. 2005, *MNRAS*, 359, 1336  
 Díaz Trigo, M., Sidoli, L., Boirin, L., & Parmar, A. N. 2012, *A&A*, 543, A50  
 Frank, J., King, A. R., & Lasota, J.-P. 1987, *A&A*, 178, 137  
 Griem, H. R. 1974, Spectral line broadening by plasmas  
 Jones, C., Forman, W., Tananbaum, H., & Turner, M. J. L. 1976, *ApJ*, 210, L9  
 Kallman, T. & Bautista, M. 2001, *ApJS*, 133, 221  
 King, A. L., Miller, J. M., Raymond, J., et al. 2012, *ApJ*, 746, L20  
 Kotani, T., Ebisawa, K., Dotani, T., et al. 2000, *ApJ*, 539, 413  
 Kubota, A., Dotani, T., Cottam, J., et al. 2007, *PASJ*, 59, 185  
 Kuulkers, E., Wijnands, R., Belloni, T., et al. 1998, *ApJ*, 494, 753  
 Lee, J. C., Reynolds, C. S., Remillard, R., et al. 2002, *ApJ*, 567, 1102  
 Madej, J. & Róžańska, A. 2004, *MNRAS*, 347, 1266  
 Miller, J. M., Raymond, J., Homan, J., et al. 2006, *ApJ*, 646, 394  
 Miller, J. M., Raymond, J., Reynolds, C. S., et al. 2008, *ApJ*, 680, 1359  
 Novikov, I. D. & Thorne, K. S. 1973, in *Black Holes (Les Astres Occlus)*, ed. C. Dewitt & B. S. Dewitt, 343–450  
 Orosz, J. A. & Bailyn, C. D. 1997, *ApJ*, 477, 876  
 Parmar, A. N., Angelini, L., & White, N. E. 1995, *ApJ*, 452, L129  
 Parmar, A. N., Oosterbroek, T., Boirin, L., & Lumb, D. 2002, *A&A*, 386, 910  
 Parmar, A. N., Stella, L., & White, N. E. 1986, *ApJ*, 304, 664  
 Ponti, G., Fender, R. P., Begelman, M. C., et al. 2012, *MNRAS*, 422, L11  
 Róžańska, A. & Madej, J. 2008, *MNRAS*, 386, 1872  
 Róžańska, A., Madej, J., & Gancarczyk, M. 2011a, in *Fast X-ray Timing and Spectroscopy at Extreme Count Rates (HTRS 2011)*  
 Róžańska, A., Madej, J., Konorski, P., & Sądowski, A. 2011b, *A&A*, 527, A47  
 Schnerr, R. S., Reerink, T., van der Klis, M., et al. 2003, *A&A*, 406, 221  
 Shakura, N. I. & Sunyaev, R. A. 1973, *A&A*, 24, 337  
 Sidoli, L., Oosterbroek, T., Parmar, A. N., Lumb, D., & Erd, C. 2001, *A&A*, 379, 540  
 Tomsick, J. A., Lapshov, I., & Kaaret, P. 1998, *ApJ*, 494, 747  
 Ueda, Y., Asai, K., Yamaoka, K., Dotani, T., & Inoue, H. 2001, *ApJ*, 556, L87  
 Ueda, Y., Inoue, H., Tanaka, Y., et al. 1998, *ApJ*, 492, 782  
 White, N. E. & Swank, J. H. 1982, *ApJ*, 253, L61

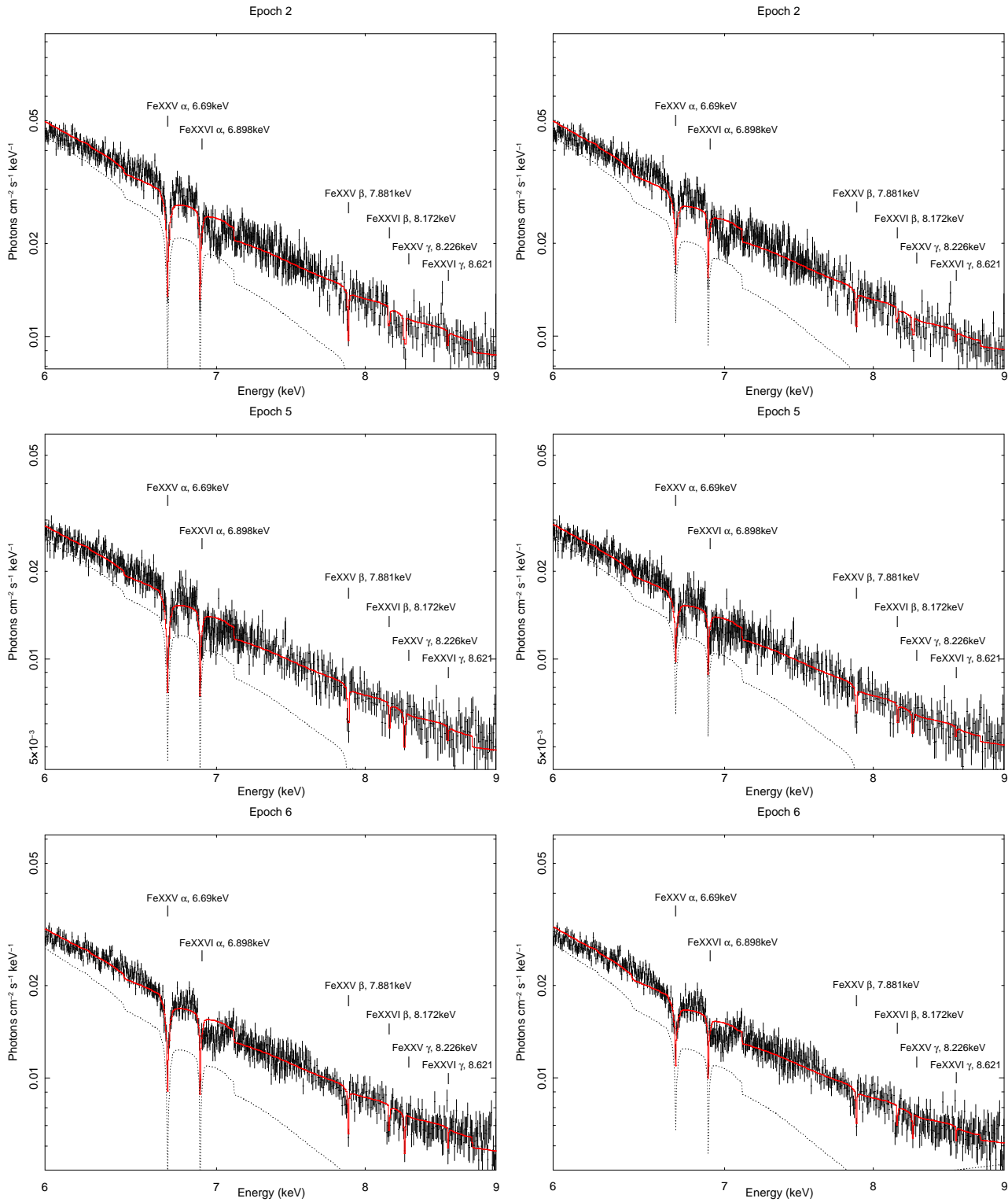


**Fig. 3.** Iron line region from 6-9 keV, where absorption features are clearly seen. Different panels represent observations for three different epochs. Black crosses show the data, black dotted lines represent  $\tau_{\text{RM}}$  model, while red solid lines show total model. Upper panels show disk seen at  $i = 11 \pm 5^\circ$ , whereas lower panels show disk seen at  $i = 70 \pm 6^\circ$ . All spectra favor fitting for  $i = 11 \pm 5^\circ$ , since modeled lines are the deepest for this model.

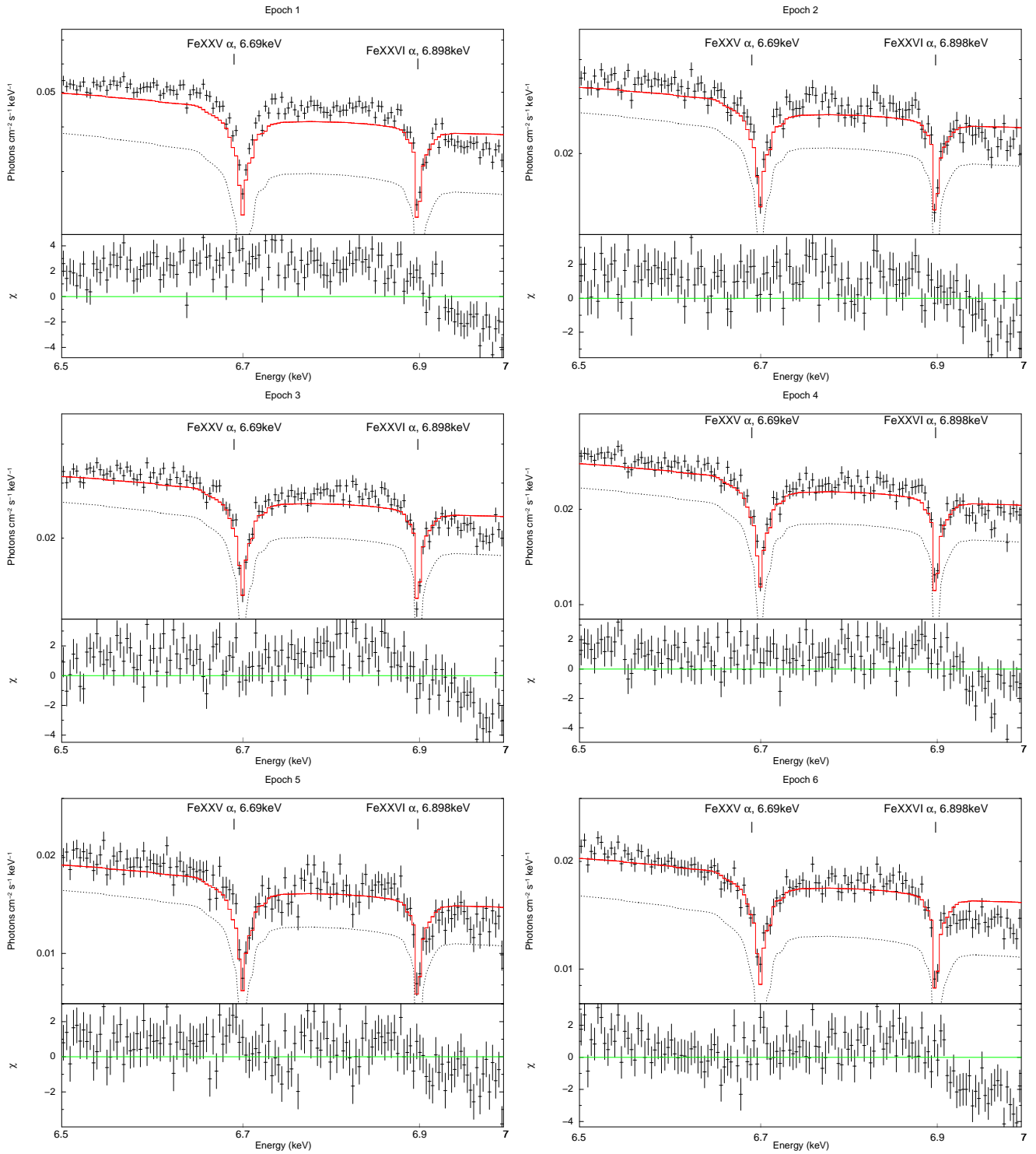


**Fig. 4.** Focus on the resonant He and H-like iron lines for the fitting done in the 6-9 keV energy range (see text for explanation). Black crosses show the data, black dotted lines represent  $\Lambda$ RM model, while red solid lines show total model. Clearly, complicated line profiles computed in our model, match the observations very well for almost each epoch. Residues are presented below each panel. Here we present spectra for  $i = 11 \pm 5^\circ$ .